Identification of Human Epididymis Protein-4 as a Novel Fibroblast-Derived Mediator of Fibrosis

Valerie S. LeBleu[1], **Yingqi Teng**[1], **Joyce T. O'Connell**[1], **David Charytan**[2], **Gerhard A Müller**[3], **Claudia A Müller**[3], **Hikaru Sugimoto**[1], and **Raghu Kalluri**[1,4,5]

[1]Division of Matrix Biology, Department of Medicine, Beth Israel Deaconess Medical Center, Boston, MA

[2]Renal Division, Department of Medicine, Brigham and Women's Hospital, Boston, MA

[3]Department of Nephrology and Rheumatology, Georg-August-University Medical Center, Göttingen, Germany

[4]Department of Biological Chemistry and Molecular Pharmacology, Harvard Medical School, Boston, MA

[5]Harvard-MIT Division of Health Sciences and Technology, Boston, MA

Abstract

The functional contribution of myofibroblasts in fibrosis is not well understood[1–3]. Using a novel genetic mouse model to track and isolate myofibroblasts, we performed gene expression profiling followed by biological validation to identify human epididymis protein 4 (*HE4*, also known as WAP 4-disulfide core domain-2 or *Wfdc2*) as the most up-regulated gene in fibrosis-associated myofibroblasts. The *HE4* gene encodes for a putative serine protease inhibitor that is upregulated in human and mouse fibrotic kidneys, and elevated in the serum of patients with kidney fibrosis. HE4 suppresses the activity of multiple proteases, including serine proteases and matrix metalloproteinases, and specifically inhibits their capacity to degrade type I collagen. In particular, we identified two novel serine proteases, Prss35 and Prss23, as HE4 targets with functional relevance in kidney fibrosis. Administration of HE4 neutralizing antibodies accelerated collagen I degradation and inhibited fibrosis in three different mouse models of renal disease. Collectively, these studies suggest that HE4 is a potential biomarker of renal fibrosis and a novel therapeutic target.

Renal fibrosis is the scarring and chronic pathological remodeling of the kidney, in which the normal tissue architecture is progressively replaced by type I collagen and other extracellular matrix (ECM) proteins[2,4,5]. Accumulation of type I collagen leads to structural

and functional alterations of the kidney parenchyma and eventual organ failure. Most chronic renal damage, irrespective of the etiology, leads to renal fibrosis—a self-perpetuating process that is likely facilitated by the recruitment of activated fibroblasts (myofibroblasts) and propagation of an inflammatory response[1,3,6]. Many previous studies have suggested a possible role for myofibroblasts in the production of scar-forming type I collagen and pathogenesis of renal fibrosis[1,6–8].

We generated mice in which the gene for red fluorescent protein was expressed under the control of *α SMA* promoter (*α SMA-RFP*) (Supplementary Fig. 1). In healthy kidneys of *α SMA-RFP* transgenic mice, αSMA+ cells were restricted to occasional rare interstitial cells and smooth muscle cells, whereas a significant increase in interstitial αSMA+ cells (10-fold increase) was detected following unilateral ureteral obstruction (UUO) (Fig. 1a). We FACS-isolated and expanded αSMA+ cells from control and fibrotic kidneys of *α SMA-RFP* transgenic mice (Fig. 1b) and performed gene expression profiling to identify candidate genes that may mediate fibrosis. Pathway analysis revealed alterations in genes associated with TGFβ-mediated cytoskeleton remodeling, mesenchymal phenotype acquisition, cell adhesion, and transport of clathrin-coated vesicles (Supplementary Fig. 2). Upregulated genes included those encoding for extracellular matrix proteins, including *Biglycan*, *Desmin* and *Decorin,* as well as serine proteases such as *Prss35* and *Prss23*, and protease inhibitors that included *SerpinF1* and *Serpin10a* (Supplementary Table 1). Interestingly, the highest upregulated gene in this array analysis (37-fold increase) was the whey acidic protein (WAP) disulfide core domain 2 or *Wfdc2* gene, encoding for the mouse homolog of human epididymis protein 4 ('HE4' is used here to highlight both mouse *Wfdc2* and human *WFDC2* gene product) (Supplementary Table 1). While many of the other top upregulated genes have been previously reported to play a role in either liver, lung, colon or kidney fibrosis (Supplementary Table 1), our expression profiling data identified *HE4* as a novel gene with potential implications for fibrosis. Real-time PCR analysis reveals a 12-fold upregulation of *HE4* in fibrosis-associated fibroblasts (FAF) (Fig. 1c). Western blot analyses detected HE4 in FAF lysates and culture media as a single band (Fig. 1d–e, Supplementary Fig 3a–b). Elevation in HE4 expression was also observed in fibrotic kidneys (Fig. 1f–g, Supplementary Fig. 3a–b).

The four-disulfide core domain repeats or WAP functional motif of HE4 suggested a protease inhibitor activity[9,10]. Serine protease activity in fibrotic kidney lysates was significantly inhibited when pre-incubated with recombinant HE4 protein (Fig. 2a). In this assay, an increase in the degradation of the substrate, BAPNA, measured using spectrophotometric detection of the released p-nitroaniline (pNA) product, indicates an increase in serine protease activity. Addition of HE4 to fibrotic kidney lysates reduced p-NA levels, indicative of its capacity to function as an inhibitor of enzymes with trypsin-like serine protease activity. The FAF and fibrotic kidney[11] gene expression profiles identified the upregulation of two serine proteases with unknown role in renal fibrosis, Prss35 and Prss23. Validation by real-time PCR reveals 3- and 1.5-fold upregulation of *Prss35*, and 2.1- and 2.5-fold upregulation of *Prss23*, in FAF and fibrotic kidneys respectively (Fig. 2b). Both Prss23 and Prss35 showed gelatinolytic activity in zymogram assay (data not shown), and HE4 specifically inhibited Prss35 and Prss23 serine protease activity and their capacity to

degrade type I collagen (Fig. 2c, d). Hydroxyproline release assay measures collagen triple helix degradation. An increase in hydroxyproline was measured when type I collagen was subjected to either Prss35 or Prss23 serine proteases (Fig. 2d). HE4 inhibited Prss35- and Prss23-mediated degradation of type I collagen (Fig. 2d). Further, inhibitory activity of HE4 on Prss35 and Prss23 was suppressed with the addition of anti-HE4 neutralizing antibodies (Fig. 2d). HE4 inhibition of trypsin was also directly evaluated and HE4 inhibited the enzyme activity of purified trypsin and its activity in fibrotic kidney lysates (Fig. 2e and Supplementary Fig. 3c). HE4 also reduced trypsin degradation of type I collagen, and anti-HE4 neutralizing antibodies reversed this action (Fig. 2f)

We next evaluated whether the ability of recombinant human MMP2 and MMP9 to degrade type I collagen could be inhibited by HE4. Hydroxyproline release assay showed that HE4 significantly suppressed the activities of MMP2 and MMP9 to degrade type I collagen (Fig. 2g). Further, we show that HE4 directly interacts with MMP2 and MMP9, as assessed by immunoprecipitation using HE4 antibodies and subsequent western blotting analysis (Fig. 2h). HE4 also inhibited the degradation of type I collagen by bacterial collagenase, a collagenase that shares an activity profile with many mammalian MMPs (Supplementary Fig. 3d).

To functionally address the role of HE4 specifically in renal fibrosis, anti-HE4 neutralizing antibody was administered to mice following UUO. Mice treated with anti-HE4 antibody showed improvement in renal fibrosis when compared to control IgG-treated mice, as demonstrated by significant decrease in Masson's trichrome staining (75% reduction) and type I collagen content (80% reduction) in the anti-HE4-treated mice (Fig. 3a). In the nephrotoxic serum-induced nephritis (NTN) mouse model, treating mice with anti-HE4 neutralizing antibody also resulted in significant reduction in Masson's trichrome staining (50% reduction) and type I collagen (60% reduction), suggestive of reduced renal fibrosis (Fig. 3a). Blood urea nitrogen and urine albumin/creatinine measurements showed that anti-HE4 treatment improved renal functions in NTN mice (Fig. 3b). Similar results were also observed in mice with 5/6 nephrectomy (Supplementary Fig. 4). Double immunolabeling for HE4 and αSMA indicated that the majority of HE4+ cells are αSMA positive (~80%). Anti-HE4-treated mice showed a significant decrease in HE4+/αSMA+ double-positive cells, compared to anti-IgG-treated mice (Fig. 3c and Supplementary Fig. 5a). Kidney lysates from UUO mice treated with anti-IgG showed an overall increase in type I collagen digestion activity when compared to kidney lysates from contralateral kidneys (Fig. 3d). Kidney lysates from UUO mice treated with anti-HE4 showed an overall decrease in type I collagen degradation activity, including a decrease in type I collagen digestion mediated by MMP2 and MMP9 as assessed by gelatin zymography (Fig. 3d). Serine proteases activity in fibrotic kidney lysates was significantly increased in comparison to non-fibrotic kidney lysates (Fig. 3e). Treatment with anti-HE4 neutralizing antibodies also reduced trypsin and trypsin-like serine protease activity in kidney lysates from treated mice when compared to kidney lysates from control mice (Fig. 3e). These results reflect an overall decrease in protease activity as a measure of improved kidney histology due to reduction in fibrosis in the anti-HE4 treated mice at the experimental endpoint (UUO Day 10).

MMP expression was evaluated by western blot analyses of normal and fibrotic kidney lysates. MMP2 and MMP9 were significantly upregulated in fibrotic kidney lysates (Fig. 3e), with no detection of MMP1, MMP3, MMP8, or MMP12 in fibrotic kidney lysates by western blotting or gelatin and casein zymography (data not shown)[12]. MMP9 protein levels were significantly reduced in kidney lysates from mice treated with anti-HE4 (Fig. 3e), again reflecting an overall decrease in fibrosis and improvement in kidney histology in the treated mice rather than a direct effect of anti-HE4 treatment on MMPs at the experimental endpoint (UUO, Day 10). In this regard, macrophage infiltration was also reduced in anti-HE4 treated mice compared with anti-IgG treated control mice (Supplementary Fig. 5b). Migration, proliferation and αSMA expression of FAF was not affected by anti-HE4 neutralizing antibody (Supplementary Fig. 5c–e). While the number of αSMA+ cells decreased in kidneys from mice treated with anti-HE4 neutralizing antibody, the relative proportion of proliferating myofibroblasts, as measured by co-localization of αSMA and Ki67 remained similar. These results suggest that the anti-HE4 neutralizing antibody treatment did not directly affect myofibroblast proliferation (Supplementary Fig. 5f).

Upregulation of HE4, PRSS35 and PRSS23 expression was observed in FAF from human fibrotic kidneys (Fig. 4a, b). Western blot analyses also revealed an upregulation of HE4 in human FAFs (Fig. 4c) and showed that HE4 is secreted by human FAF (Fig. 4d). Immunolabeling studies further revealed renal interstitial as well as tubular expression of HE4 in human fibrotic kidneys (Fig. 4e). Additionally, serum levels of HE4 were significantly elevated in patients with chronic renal disease with biopsy-confirmed fibrosis (~600pM) when compared to control serum from healthy individuals (~180pM) (Fig. 4f and Supplementary Table 2).

HE4 gene encodes for a highly conserved WAP domain-containing protein suggestive of a putative serine protease inhibitor activity[9,10,13–15]. The protein is implicated in sperm maturation[9] and potentially has a role in natural immunity[16], but the biological function of HE4 is unknown. Interestingly, it was identified as the most upregulated gene in fibrotic kidneys of dogs[17]. HE4 was also reported to be significantly upregulated in fibrotic kidneys of mice[11,18], and its transcript level in human kidney transplant biopsies was found to be strongly correlated with low eGFR[19]. Despite these observations, the role of HE4 in renal fibrosis and its putative serine protease activity remained unexplored. WFDC domain protein family members, with suspected antimicrobial and protease inhibitor activities (via its four-disulfide core domain repeats or WAP motifs), were initially described to be exclusively transcribed in the epididymis but was later identified to be also expressed in other regions of the male and female reproductive tract, kidney, respiratory tract and several tumor cell lines, including ovarian, colon, breast and renal cell lines[13,20,21].

Here we show that HE4 is robustly expressed by myofibroblasts and its concentration in the serum of patients with kidney diseases correlates with renal fibrosis and may therefore serve as a novel biomarker to predict fibrosis. A large-scale patient analysis is warranted to further validate these preliminary findings. In this regard, a serum HE4 (sHE4) detection test recently received FDA clearance to aid in diagnosis and monitoring recurrence and progression of ovarian cancer, and high level of sHE4 is a prognostic indicator and identifies high-risk serous and endometrial cancer patients[22,23].

Our study identifies two new specific serine proteases (*Prss23* and *Prss35*) as significantly upregulated in kidney fibrosis, which appear to act, at least in part, as type I collagen degrading enzymes and targets of HE4 protease inhibition. In this regard, TIMPs and other inhibitors such as PAI-1 have been studied for their role in the pathogenesis of organ fibrosis[24–26]. We also demonstrate that HE4 can inhibit MMP2/9-induced degradation of type I collagen, which can be reversed by the use of a neutralizing antibody to HE4. While the activity of both MMP2 and MMP9 (and other proteins with type I collagen degrading activities) was significantly reduced by HE4, the overall MMP9 protein levels were also reduced in anti-HE4 treated mice. Such drop in MMP9 levels could also reflect a secondary effect of the anti-HE4 treatment in resolving overall fibrosis and its associated inflammation. HE4 emerges as a potential pan-serine protease inhibitor, with a possible role for a significant downregulation of serine protease activity in fibrotic kidneys. We speculate that such pan-protease inhibitory activity promotes a pro-fibrotic process by inhibiting a number of enzymes that contribute to type I collagen turnover in the fibrotic kidney. Indeed, renal fibrosis in three different models can be inhibited by systemic administration of HE4-specific neutralizing antibody. Collectively, our studies identify HE4 as a novel biomarker for detection of renal fibrosis and as a target to inhibit renal fibrosis.

Methods

Animal studies

αSMA-RFP transgenic mice were generated in our laboratory (see supplementary material and methods). Unilateral ureteral obstruction (UUO) was performed and the mice were euthanized 10 days later. Nephrotoxic serum was injected to induce nephrotoxic serum nephritis (NTN) as previously described[27]. For rabbit anti-HE4 antibody injections in mice with UUO, 14mg/Kg BW of antibody (Epitomics, 3423-1) was administered i.p. every other day for 10 days. Rabbit IgG control antibody (Epitomics) was also given at 14mg/Kg BW i.p. every other day for 10 days. For anti-HE4 and IgG control antibody injection in mice with NTN received treatment starting 4 weeks after nephrotoxic serum injection until they were euthanized 2 weeks later (6 weeks after nephrotoxic serum) at the same dose, route, and schedule as described above. All mice used for UUO experiment were on Balb/C genetic background (n=5 in each group). All mice for NTN were on CD1 background (n=6 (anti-HE4) and n=5 (anti-IgG). All mice were housed under standard conditions at the Beth Israel Deaconess Medical Center animal facility. All animal procedures were reviewed and approved by the Animal Care and Use Committee of the Beth Israel Deaconess Medical Center.

Cell Culture

Primary mouse contralateral kidney normal fibroblasts (NF) and UUO kidney fibrosis-associated fibroblasts (FAF) were cultured from αSMA-RFP mice 10days following UUO. Briefly, the kidneys were harvested and minced and allowed to digest in 300U/ml Type IV collagenase in Dulbecco's Modified Eagle's Medium, 10% fetal bovine serum, and penicillin and streptomycin (each 100U/ml) (cDMEM) overnight at 37°C and 5% CO_2. The next day the digested tissue pieces are centrifuged (RT, 1500rpm) and resuspended in cDMEM and allowed to reach confluence while incubating at 37°C and 5% CO_2. The FACS

purified and in culture expanded RFP$^+$ cells were compared for consistency and purity. The human fibroblast cell lines (NF1-3 and FAF1-5) were obtained and cultured as previously described[28].

Quantitative Real time PCR analysis

Kidneys (Day 10 following UUO) and fibroblasts (from kidneys at day 10 following UUO) were homogenized in TRIzol® (Invitrogen), extracted according to the manufacturer's directions, and cDNA synthesis was performed using Applied Biosystem cDNA synthesis kit according to the manufacturer's directions. Real-time PCR was carried out for mouse *Col1a1, Acta2 (α SMA), Prss23, Prss35,* and mouse and human HE4 and reactions were carried out in technical triplicates. Primer sequences can be found in supplementary information. Primers were utilized with SYBR Green PCR Master Mix in a 7300 Sequence Detector System (Applied Biosystems) and measurements were standardized to expression of the β-actin housekeeping gene (mouse) or β2-microglobulin house-keeping gene (human). Relative gene expression is reported by normalizing to healthy contralateral kidneys (Fig. 2b), non-fibrotic mouse kidney fibroblasts (NF, Fig. 2b) or non-fibrotic human fibroblast (TK173 (NF1), Fig. 4a), or the average of 3 non-fibrotic human fibroblasts (NF1-3, Fig. 4b), which were arbitrarily set to 1.

Gelatin zymography was performed as previously described[12]. Kidney lysates (20μg) were used as substrate and HT1080 cell lysates (20μg) were used as positive control. Relative band densities for MMP2 and MMP9 digest were analyzed using ImageJ gel analyser software and normalized to band densities of actin.

Hydroxyproline release assay

Activated recombinant human MMP2 and MMP9 (R&D Systems), or Prss23/Prss35 (Novus Biologicals), or trypsin (Invitrogen) with or without recombinant human HE4 protein (5μg Sino Biological Inc.), and with or without anti-HE4 antibody (4μg, from Epitomics), were incubated with 1mg of type I collagen (Sigma) in 1ml collagenase buffer (100mM TRIS pH7.5; 1mM CaCl2) at 37°C under gentle agitation. 200μl of the reaction was then incubated with 300μl of Chloramine T reagent (0.056M in acetate-citrate buffer pH6.5) overnight at room temperature under gentle agitation. The mixture was then incubated for 5 hours with 500μl of Ehrlich's reagent (1M in n-propanol/perchloric acid (2:1 v/v)). The absorbance of the purple complex formed was measured at 550nm using a standard spectrophotometer. The experiment was performed in triplicate. Hydroxyproline standards were used to calculate free hydroxyproline release. Bacterial collagenase (type I collagenase, Worthington), with or without bovine serum albumin (BSA) (5μg), with or without recombinant HE4 protein, was also subjected to hydroxyproline release assay as described above.

Trypsin and serine protease activity assays

Trypsin activity was assessed using the trypsin colorimetric assay (Abcam) and serine protease activity was measured using N-Benzoyl-L-arginin 4-nitroanilide hydrochloride (BAPNA, 1mM in 100mM Tris pH 8.5) as substrate as previously described changing the incubation time at 37°C to 24 hours[29].

Histological processing, light microscopy, and morphometric analyses

All procedures were performed as previously described[30,31].

Renal function analyses

Blood Urea Nitrogen (BUN) levels and albuminuria were measured as previously described[31,32]. The ratio of urine albumin over urine cretatinine is expressed as μg of urine albumin over μg of urine cretatinine.

Immunohistochemistry

Kidneys were fixed in 10% neutral buffered formalin, dehydrated, and embedded in paraffin. The deparaffinised sections were incubated in 10mM citrate buffer (pH 6.0) for 1 hour at boiling temperature prior blocking with 1% BSA in TBS for 30 min. The sections were immunolabeled using anti-Collagen I antibody (Southern Biotech) overnight at 4°C. The immunobound antibodies were detected using biotin-conjugated secondary antibodies and ABC reagent (Vector Laboratories) and the sections were developed by DAB staining and counterstained with haematoxylin. The number of DAB+ (brown) cells was analyzed in 8 visual fields from each kidney section by NIH ImageJ analysis software and double-blind cell counting using light microscopy.

Immunostaining

Frozen section of harvested kidneys embedded in O.C.T. medium were immunostained using antibodies against αSMA (Sigma), HE4 (Epitomics), Ki67 (Abcam), and F4/80 (Hyclone), and secondary fluorescent antibodies. Positive staining was quantified in 8 fields using NIH-ImageJ software and double-blind cell counting under the microscope. Pictures were taken using the Axioskop 2 fluorescent microscope, AxioCam HRC camera and the Axiovision 4.3 software.

RFP visualization

Mouse kidneys were fixed in 4% PFA overnight at 4°C and equilibrated in 30% sucrose overnight at 4°C. The kidneys were then embedded in OCT compound and frozen sections (5μm) were mounted with Vectashield Mounting Medium with DAPI (Vectashield) and a glass coverslip and visualized under RFP fluorescent filter.

Western Blot analysis and Immunoprecipitation (IP)

Kidneys and cells were homogenized in lysis buffer (1%TritonX100, 0.1%SDS, 150mM NaCl, 50mM Tris-HCL(pH7.5), 1%NaDOC,) supplemented with protease cocktail inhibitor(Roche) and denatured with SDS-Laemmli buffer with 5% β-mercaptoethanol. Protein concentration was measured using BCA assay. For immunoprecipitation, fibrotic kidney lysates (500μg) were pre-cleared with protein A/G beads only O/N at 4°C then incubated with anti-IgG or anti-HE4 O/N at 4°C with protein A/G beads. The beads were washed 5 times before the proteins were eluted in Laemmli sample buffer by boiling 5 minutes. For western blot analyses, 20μg of lysates, or 50μl of culture media (of 200,000 seeded cells), or ~500ng of recombinant HE4 were resolved by SDS-PAGE and transferred onto immobilon-P-membrane (Millipore Corporation, Bedford, MA) and blocked in 5% dry

milk in TBS-T (TBS pH 7.6, 0.1% tween20). The membranes were blotted against HE4 (Epitomics), MMP2 (Cell signaling), MMP9 (Cell signaling) or actin (Sigma), diluted as recommended by the manufacturer. Relative band densities for MMP2 and MMP9 were analyzed using ImageJ gel analyser software and normalized to band densities of actin.

Human tissue, sera, and fibroblasts lines

Human tissue and sera were provided by Dr. David Charytan (Renal Division, Department of Medicine, Brigham and Women's Hospital, Boston, MA) under appropriate patient consent and institutional approval. Human fibroblast lines were provided by Drs. Gerhard Müller and Claudia Müller (Department of Nephrology and Rheumatology, Georg-August-University Medical Center, Göttingen, Germany) and were cultured as previously described[28]. The specific lines listed below used in this study were also previously described[28]. Fibrosis associated fibroblast (FAF)1: TK274, FAF2: TK188, FAF3: TK239, FAF4: TK261, FAF5: TK257. Normal fibroblasts: TK173, TK231a and TK163. The FAF6 line was derived from a de-identified kidney biopsy from a patient with Alport Syndrome and biopsy validated interstitial renal fibrosis (FAF6).

HE4 ELISA

Fifty microliters of patient sera and recombinant HE4 protein standards were mixed with 50μl of 200mM bicarbonate/carbonate buffer and the mixture was incubated overnight at 4°C in high affinity binding 96-well ELISA plates (100μl per well). Following antigen binding, the wells were blocked with 200μl blocking buffer (5% BSA in PBS), and washed twice with PBS. 100ul of 1:500 dilution of anti-HE4 antibody (Epitomics) in 1%BSA/PBS was added per well for 30minutes at room temperature. The plate was washed twice with PBS and incubated 30minutes at room temperature with 100μl of 1:4000 dilution of HRP conjugated anti-rabbit IgG antibody in 1%BSA/PBS. The plate was washed three times with PBS and developed using TMB peroxidase substrate. The reaction was stopped with 1M phosphoric acid and the absorbance values of each well read at 450nm using a standard spectrophotometer.

Supplementary Material

Refer to Web version on PubMed Central for supplementary material.

Acknowledgments

References

1. Zeisberg M, Strutz F, Muller GA. Role of fibroblast activation in inducing interstitial fibrosis. Journal of nephrology. 2000; 13 (Suppl 3):S111–120. [PubMed: 11132027]

2. Eddy AA. Molecular insights into renal interstitial fibrosis. J Am Soc Nephrol. 1996; 7:2495–2508. [PubMed: 8989727]

3. Strutz F, Muller GA. Renal fibrosis and the origin of the renal fibroblast. Nephrol Dial Transplant. 2006; 21:3368–3370. [PubMed: 16887850]

4. Okada H, Strutz F, Danoff TM, Kalluri R, Neilson EG. Possible mechanisms of renal fibrosis. Contributions to nephrology. 1996; 118:147–154. [PubMed: 8744052]

5. Zeisberg M, Neilson EG. Mechanisms of tubulointerstitial fibrosis. J Am Soc Nephrol. 21:1819–1834. [PubMed: 20864689]

6. Meran S, Steadman R. Fibroblasts and myofibroblasts in renal fibrosis. Int J Exp Pathol. 92:158–167. [PubMed: 21355940]

7. Barnes JL, Glass WF 2nd. Renal interstitial fibrosis: a critical evaluation of the origin of myofibroblasts. Contributions to nephrology. 169:73–93. [PubMed: 21252512]

8. Grgic I, Duffield JS, Humphreys BD. The origin of interstitial myofibroblasts in chronic kidney disease. Pediatr Nephrol.

9. Kirchhoff C. Molecular characterization of epididymal proteins. Rev Reprod. 1998; 3:86–95. [PubMed: 9685187]

10. Kirchhoff C, Habben I, Ivell R, Krull N. A major human epididymis-specific cDNA encodes a protein with sequence homology to extracellular proteinase inhibitors. Biol Reprod. 1991; 45:350–357. [PubMed: 1686187]

11. Hahm K, et al. Alphav beta6 integrin regulates renal fibrosis and inflammation in Alport mouse. The American journal of pathology. 2007; 170:110–125. [PubMed: 17200187]

12. Zhang G, et al. Urokinase receptor deficiency accelerates renal fibrosis in obstructive nephropathy. J Am Soc Nephrol. 2003; 14:1254–1271. [PubMed: 12707394]

13. Bingle L, Singleton V, Bingle CD. The putative ovarian tumour marker gene HE4 (WFDC2), is expressed in normal tissues and undergoes complex alternative splicing to yield multiple protein isoforms. Oncogene. 2002; 21:2768–2773. [PubMed: 11965550]

14. Clauss A, Lilja H, Lundwall A. A locus on human chromosome 20 contains several genes expressing protease inhibitor domains with homology to whey acidic protein. Biochem J. 2002; 368:233–242. [PubMed: 12206714]

15. Clauss A, Lilja H, Lundwall A. The evolution of a genetic locus encoding small serine proteinase inhibitors. Biochem Biophys Res Commun. 2005; 333:383–389. [PubMed: 15950183]

16. Bingle L, et al. WFDC2 (HE4): a potential role in the innate immunity of the oral cavity and respiratory tract and the development of adenocarcinomas of the lung. Respir Res. 2006; 7:61. [PubMed: 16600032]

17. Greer KA, et al. Gene expression analysis in a canine model of X-linked Alport syndrome. Mamm Genome. 2006; 17:976–990. [PubMed: 16964446]

18. Bielesz B, et al. Epithelial Notch signaling regulates interstitial fibrosis development in the kidneys of mice and humans. J Clin Invest. 2010; 120:4040–4054. [PubMed: 20978353]

19. Bunnag S, et al. Molecular correlates of renal functions in kidney transplant biopsies. J Am Soc Nephrol. 2009; 20:1149–1160. [PubMed: 19389845]

20. Galgano MT, Hampton GM, Frierson HF Jr. Comprehensive analysis of HE4 expression in normal and malignant human tissues. Mod Pathol. 2006; 19:847–853. [PubMed: 16607372]

21. Sivashanmugam P, et al. Characterization of mouse Eppin and a gene cluster of similar protease inhibitors on mouse chromosome 2. Gene. 2003; 312:125–134. [PubMed: 12909348]

22. Bignotti E, et al. Diagnostic and prognostic impact of serum HE4 detection in endometrial carcinoma patients. Br J Cancer. 104:1418–1425. [PubMed: 21468050]

23. Drapkin R, et al. Human epididymis protein 4 (HE4) is a secreted glycoprotein that is overexpressed by serous and endometrioid ovarian carcinomas. Cancer Res. 2005; 65:2162–2169. [PubMed: 15781627]

24. Matsuo S, et al. Multifunctionality of PAI-1 in fibrogenesis: evidence from obstructive nephropathy in PAI-1-overexpressing mice. Kidney Int. 2005; 67:2221–2238. [PubMed: 15882265]

25. Oda T, et al. PAI-1 deficiency attenuates the fibrogenic response to ureteral obstruction. Kidney Int. 2001; 60:587–596. [PubMed: 11473641]

26. Catania JM, Chen G, Parrish AR. Role of matrix metalloproteinases in renal pathophysiologies. Am J Physiol Renal Physiol. 2007; 292:F905–911. [PubMed: 17190907]

27. Zeisberg M, et al. Bone morphogenic protein-7 inhibits progression of chronic renal fibrosis associated with two genetic mouse models. Am J Physiol Renal Physiol. 2003; 285:F1060–1067. [PubMed: 12915382]

28. Bechtel W, et al. Methylation determines fibroblast activation and fibrogenesis in the kidney. Nature medicine. 16:544–550.

29. Panicker LM, Usha R, Roy S, Mandal C. Purification and characterization of a serine protease (CESP) from mature coconut endosperm. BMC Res Notes. 2009; 2:81. [PubMed: 19426537]

30. LeBleu V, Sugimoto H, Miller CA, Gattone VH II, Kalluri R. Lymphocytes are Dispensable for Glomerulonephritis but Required for Renal Interstitial Fibrosis in Matrix Defect Induced Alport Renal Disease. Laboratory Investigation. 2008:xx. in press.

31. Lebleu V, et al. Stem Cell Therapies Benefit Alport Syndrome. J Am Soc Nephrol. 2009

32. Sugimoto H, et al. Activin-like kinase 3 is important for kidney regeneration and reversal of fibrosis. Nature medicine. 2012; 18:396–404.
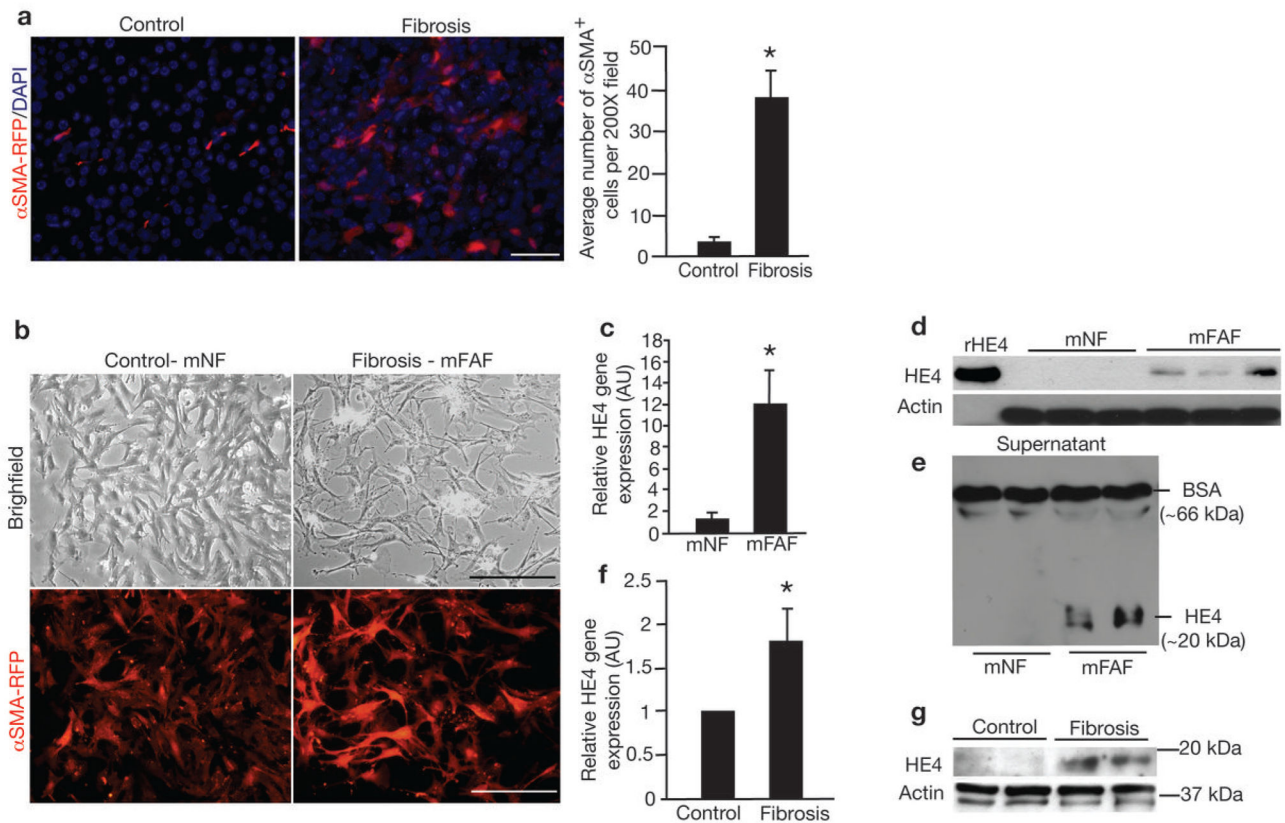
Figure 1. αSMA+ myofibroblasts accumulate in the interstitium and express HE4 in renal fibrosis

a. Visualization of αSMA-RFP+ cells in control (contralateral kidney to UUO) and fibrotic mouse kidneys (UUO) from *α SMA-RFP* transgenic mice. DAPI (blue): nuclei. Quantitation of αSMA+ cells per visual field in control and fibrotic kidney, evaluated at Day 10 post UUO. **b.** Visualization of αSMA-RFP+ myofibroblasts cultured from control kidneys (mouse normal fibroblasts, mNF) and fibrotic kidneys (mouse fibrosis-associated fibroblasts, mFAF). **c**. Relative HE4 gene expression in mFAF normalized to mNF. AU: Arbitrary Unit. **d**. Western blot for HE4 in mouse mNF and mFAF. Actin was used as an internal control. rHE4: recombinant HE4 protein used as positive control. **e**. Western blot for HE4 in mNF and mFAF culture media, with loading normalized to cell numbers. Bovine serum albumin (BSA) also controls for lane loading. **f**. Relative HE4 gene expression in control kidneys (n=5) and fibrotic kidneys (n=5), evaluated at Day 10 post UUO. **g**. Western blot for HE4 in mouse control and fibrotic kidneys. Actin was used as an internal control. Scale bar: 50μm. Data shown as mean +/− sem. *$p < 0.05$.
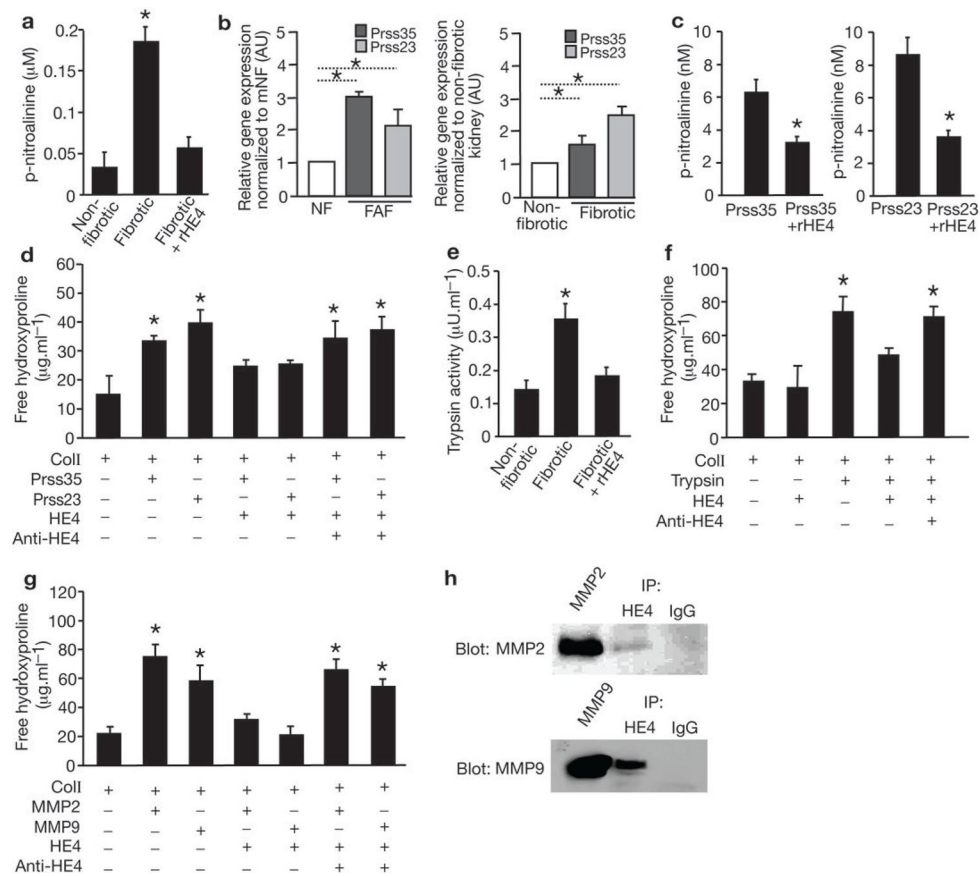
Figure 2. HE4 is a pan-serine protease and MMP2/9 inhibitor which prevents type I collagen degradation

a. p-nitroalinine release in nM assessed by spectrophotometric readout of color development as a measure of serine protease activity in non-fibrotic control kidney lysates, fibrotic kidney lysates (UUO, Day 10), and fibrotic kidney lysates (UUO, Day 10) incubated with recombinant HE4 protein (rHE4). **b**. Relative *Prss23* and *Prss35* gene expression in mouse fibrosis-derived fibroblasts (mFAF) and mouse fibrotic kidneys (Fibrotic) compared and normalized to mouse normal fibroblasts (mNF, derived from non-fibrotic kidneys) and contralateral non-fibrotic kidneys (evaluated at Day 10 post UUO), respectively. nNFs and contralateral non-fibrotic kidneys were set arbitrarily to 1 (white bar). AU, arbitrary units. **c**. p-nitroalinine release in nM assessed by spectrophotometric readout of color development using Prss23 and Prss35 serine protease with and without recombinant HE4 (rHE4). **d**. Hydroxyproline release assay: free hydroxyproline ($\mu g.ml^{-1}$) from type I collagen digestion: type I collagen digested by Prss23 or Prss35 with and without rHE4, with and without anti-HE4 antibody. **e**. Trypsin activity in non-fibrotic control kidney lysates, fibrotic (UUO, Day 10) kidneys, and fibrotic kidneys pre-treated with rHE4. **f.** Hydroxyproline release assay: free hydroxyproline ($\mu g.ml^{-1}$) from type I collagen digestion: type I collagen digested by trypsin with and without HE4, with and without BSA, and with and without anti-HE4 antibody. **g.** Hydroxyproline release assay: free hydroxyproline ($\mu g.ml^{-1}$) from type I collagen digestion: type I collagen digested by MMP2 or MMP9 with and without rHE4, with and without anti-HE4 antibody. **h.** Immunoprecipitation (IP) of fibrotic kidney lysates

using IgG (control) or HE4 antibody and western blot for MMP2/9. Data shown as mean +/− sem. *p<0.05.
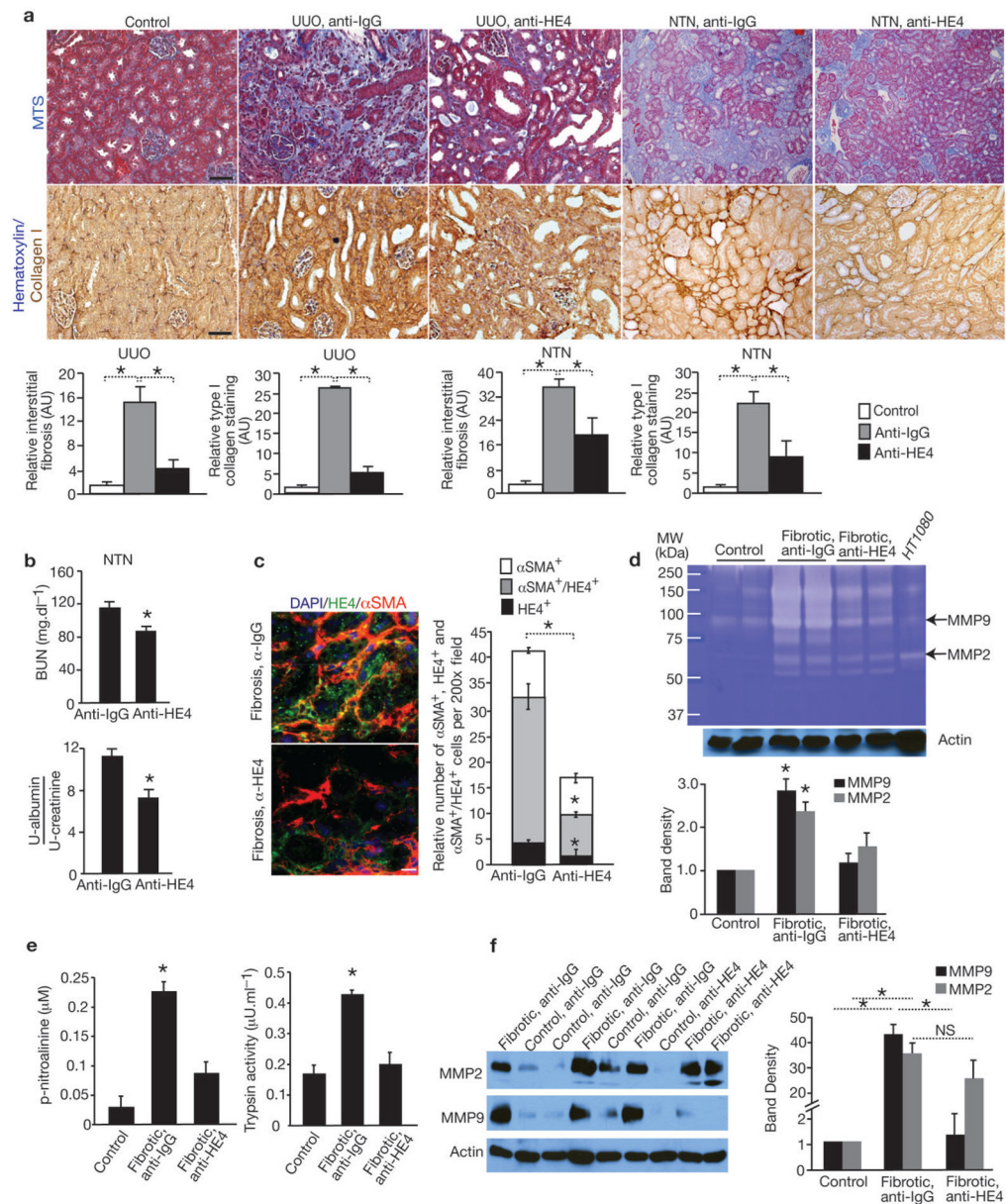
Figure 3. HE4 neutralization inhibits kidney fibrosis

a. Representative Masson Trichrome (MTS) and type I collagen staining of control and fibrotic kidneys from mice treated with anti-HE4 (UUO: n=5, NTN: n=6) or anti-IgG (UUO: n=5, NTN: n=5) antibody. Respective morphometric analyses for relative interstitial fibrosis based on MTS staining and type I collagen staining shows reduced fibrosis in anti-HE4-treated mice. AU: Arbitrary Unit. **b**. Blood urea nitrogen (BUN, mg.dL^{-1}) and urine albumin/creatinine ratio measurements of mice with NTN and treated with anti-IgG (n=5) or anti-HE4 (n=6) antibodies. **c**. Immunolabeling for HE4 and αSMA in fibrotic kidneys from mice treated with anti-HE4 or anti-IgG control antibodies. DAPI (blue): nuclei. Histogram represents the relative number of αSMA$^+$, HE4$^+$, αSMA$^+$/HE4$^+$ (double positive) cells per field of view. **d.** Gelatin zymography using lysates of contralateral (normal) kidney, fibrotic

kidneys of mice treated with anti-IgG, and fibrotic kidneys of mice treated with anti-HE4. Lysates are from kidneys at Day 10 post UUO. Histogram depicts relative band intensity normalized to actin western blot of samples loaded. **e**. Serine protease activity in kidney lysates (UUO) from fibrotic kidneys and fibrotic kidneys of mice treated with anti-HE4 (left). Trypsin activity in kidney lysates (UUO) from fibrotic kidneys and fibrotic kidneys of mice treated with anti-HE4 (right). Lysates are from kidneys at Day 10 post UUO. **f.** Western blot analyses for MMP2, MMP9 and actin loading control of lysates of contralateral (normal) kidney of mice treated with anti-IgG or anti-HE4 and of fibrotic kidneys of mice treated with anti-IgG or anti-HE4. Lysates are from kidneys at Day 10 post UUO. Histogram depicts relative band intensity normalized to actin. Scale bar: 50μm. Data shown as mean +/− sem. *p<0.05.
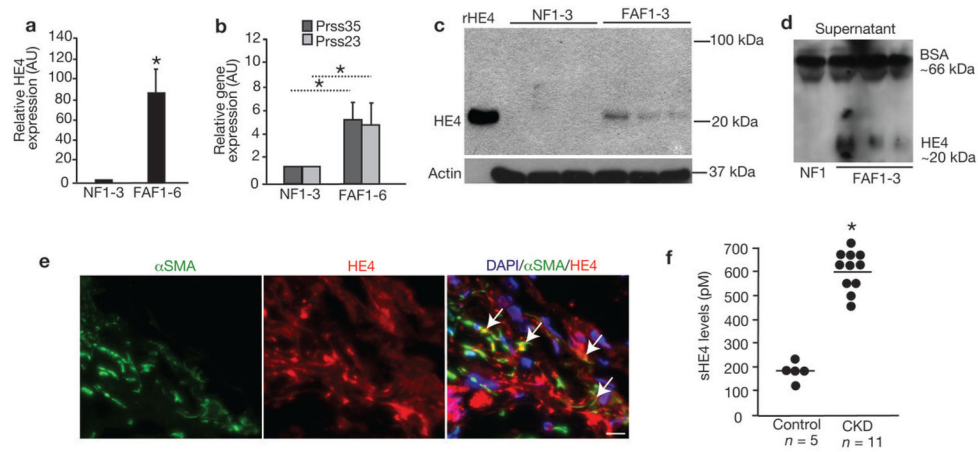
Figure 4. HE4 is elevated in human fibrotic kidneys, human fibrosis-associated fibroblasts and in serum of patients with renal fibrosis

a. Relative HE4 gene expression of different fibroblast cultures (normalized to normal fibroblast (NF, line TK173) set arbitrarily to 1). Fibrosis associated fibroblast (FAF) 1: TK274, FAF2: TK188, FAF3: TK239, FAF4: TK261, FAF5: TK257. AU, arbitrary units. **b**. Relative *PRSS23* and *PRSS35* gene expression of different fibroblast cultures (normalized to normal fibroblast (NF, line TK173) set arbitrarily to 1). AU, arbitrary units. **c.** Western blot analysis for HE4 in human NF (from left to right: line TK173, TK231a and TK163) and human FAF (from left to right line TK274, TK188, and TK239). Actin is used as internal control. **d.** Western blot for HE4 in human NF and FAF culture media, with loading normalized to cell numbers. Bovine serum albumin (BSA) also controls for lane loading. **e**. Immunolabeling for HE4 and αSMA in human kidneys with chronic kidney disease (Alport syndrome) and renal fibrosis. DAPI (blue): nuclei. **f**. Serum HE4 (sHE) levels (pM) from healthy control (n=5) and CKD patients (n=11). Scale bar: 50μm. *p<0.05